Journal of Renewable Energy and Environment

Research Article

Journal Homepage: www.jree.ir

Effect of Covering Aperture of Conical Cavity Receiver on Thermal Performance of Parabolic Dish Collector: Experimental and Numerical Investigations

Sina Eterafi [a], Shiva Gorjian [a*], Majid Amidpour [b]

[a] *Department of Biosystems Engineering, Factuly of Agriculture, Tarbiat Modares University (TMU), P. O. Box: 14115-111, Tehran, Tehran, Iran.*
[b] *Department of Energy System Engineering, Factuly of Mechanical Engineering, K. N. Toosi University of Technology, P. O. Box: 19395-1999, Tehran, Tehran, Iran.*

PAPER INFO

Paper history:
Received 06 April 2021
Accepted in revised form 10 August 2021

Keywords:
Experimental Analysis,
Conical Cavity Receiver,
Ultra-White Glass Cover,
Parabolic Dish Concentrator

ABSTRACT

In this study, the effect of covering the aperture area of a conical cavity receiver with an ultra-white glass on operational parameters of a Parabolic Dish Collector (PDC) was numerically and experimentally investigated under climate conditions of Tehran (35.44° N latitude and 51.10° longitude). The main components of the experimental setup include a dish reflector, a conical cavity receiver, Heat Transfer Fluid (HTF), hydraulic and cooling cycle, and a sun tracker. For this purpose, a conical cavity receiver with an ultra-white glass cover on its aperture was numerically modeled in Fortran software. During the evaluation, environmental parameters including ambient temperature, solar radiation, and wind speed were considered as inputs of the model. The results revealed fair agreement between the numerical and experimental data with the maximum error of approximately 4.63 % and 7.89 % for receivers with and without the glass cover on the aperture, respectively. For a steady-state analysis, the mean values of useful energy ($\dot{Q}_u$) absorbed by the receiver were calculated as 1,253.25 W and 987.68 W, while thermal efficiency (η_{th}) of the receiver was calculated as 52.61 % and 40.69 % for receivers with and without glass cover, respectively. The results revealed that both η_{th} and $\dot{Q}_u$ followed a similar trend of the variations in the HTF's temperature between the inlet and outlet of the receiver. Also, the overall heat loss coefficient (U_l) and the collector heat removal factor (F_r) were calculated as 420.76 W/m^2°C and 0.62 for the conical cavity receiver with the glass cover.

https://doi.org/10.30501/jree.2021.275871.1194

1. INTRODUCTION

Solar energy is the most abundant and freely available renewable energy source. In geographical regions with higher potential of solar energy, this renewable source can be considered as the best alternative to fossil fuels in distributed generation systems [1, 2]. Harnessing solar energy using thermal devices such as collectors and concentrators can be done in various applications including electric power generation systems, heating and cooling applications, cogeneration and direct thermal applications, desalination, and thermochemical operations [3-5]. Parabolic Dish Concentrators (PDCs) offer higher thermal performance than other solar collectors due to their high concentration ratio and employing two-axis tracking systems, causing them to achieve a high temperature range up to 1200 °C [6-8]. The most important component of PDCs which has been widely evaluated in the literature is the receiver. In a PDC, to achieve high temperature ranges, reducing the heat loss of the receiver is of particular importance. Also, among different types of receivers employed in PDCs including external, cavity, and flat, the efficiency of the cavity has been reported as the highest one with the lowest level of heat loss [9-11]. Different values of thermal efficiencies have been reported for cavity receivers due to their different geometries and shapes. According to the literature, cylindrical, conical, hemispherical, and cubical have been reported as the most common types of cavity receivers employed in PDCs [12]. In this regard, several studies have been conducted to improve the thermal performance of PDCs and their embedded components as a whole.

1.1. Literature review

Pavlovic et al. [13] conducted numerical and experimental investigations to evaluate the thermal performance of a flat spiral tube receiver. In this study, numerical results were compared with the experimental data obtained from a conical cavity receiver. They concluded that the heat loss rate from a flat spiral tube receiver was much higher than that of a cavity receiver with an efficiency of about 34 %. Li et al. [14] developed a numerical Computational Fluid Dynamic (CFD) model to investigate the thermal efficiency of a conical cavity receiver employed in a heliostat system. They reported that at the constant flow rate of Heat Transfer Fluid (HTF), changes in the temperature for the inlet and outlet of the receiver from 81 K to 181 K would lead in the thermal efficiency from 39 %

*Corresponding Author's Email: gorjian@modares.ac.ir (Sh. Gorjian)
URL: https://www.jree.ir/article_134895.html

Please cite this article as: Eterafi, S., Gorjian, Sh. and Amidpour, M., "Effect of covering aperture of conical cavity receiver on thermal performance of parabolic dish collector: Experimental and numerical investigations", ***Journal of Renewable Energy and Environment (JREE)***, Vol. 8, No. 4, (2021), 29-41. (https://doi.org/10.30501/jree.2021.275871.1194).

to 60 %. Alhsani and Al-Dulaimi [15] performed an experimental comparative study of three geometries of conical, oval, and cylindrical receivers. The study was performed at three levels of flow rate and five levels of the HTF's temperature at the inlet of the receiver. It was observed that the conical cavity receiver had the maximum energy and exergy efficiencies of 82.1 % and 23.76 %, respectively. Pavlovic et al. [16] performed both experimental and numerical studies for two cavity receivers with the shapes of flat, spiral and conical and the results were compared. They also optimized the location of the receiver at the focal point of the PDC. It was observed that the conical cavity receiver had an optical efficiency of 1.38 % at the surface temperature of 200 °C with energy and exergy efficiencies of 40.45 % and 42.06 %, respectively, which was higher than those of the flat spiral receiver. In different studies, Daabo et al. [17-19] investigated three cylindrical, spherical, and conical cavity receivers by performing a numerical study using the CFD method and compared the obtained results. These studies investigated the effects of the helical tube, covering the aperture of the receiver with clear glass, and environmental parameters on the performance of the receivers. Results indicated that the optical efficiency of the conical cavity receiver was 8 % and 13 % and thermal efficiency was 8 % and 15 % higher than those of the cylindrical and spherical receivers, respectively. They also reported about a 7 % increase in thermal efficiency when the receiver aperture was covered with glass.

Azzouzi et al. [20] performed experimental and numerical investigations of cylindrical cavity receivers with an outer concrete insulation layer considering zero thermal losses from the insulated surface. In this study, the effects of the inclination angle of the receiver and variations in the Nusselt number (Nu) of wind streams on the heat loss of the interior wall of the cavity were investigated. The numerical results pointed to good agreement with a maximum 12 % deviation from the results obtained from experimental investigations. Loni et al. [21] performed both experimental and numerical studies for two cubical cavity receivers and the obtained results were compared with those obtained from cylindrical and cubical receivers. They concluded that the cubical cavity receiver offered about 9 % more thermal performance than the cylindrical receiver. Singh and Kumar Natarajan [22] compared the results of numerical models of two modified conical and hemispherical receivers models using Comsol software. It was observed that with the modified shape of the receiver aperture, the highest efficiency of 84.7 % was obtained for the conical receiver. Yuan et al. [23] performed both numerical and experimental studies and compared a type of cavity receiver with a convex end surface with a simple type of receiver. It was observed that the thermal efficiency of the receiver with the convex end surface was 6.02 % higher than that of the simple type. Bopche et al. [24] conducted an experimental study and compared a semi-spherical modified hollow receiver with its simple type. In this study, conical blades were used on the inner surface of the cavity to absorb more heat. It was observed that the thermal efficiency of the modified receiver increased by 23.5 %.

Bellos et al. [25] performed a numerical comparative study using the CFD method to achieve optimal geometry and maximum thermal efficiency of cylindrical, conical, spherical, cubical, and cylindro-conical receivers. They considered the diameter, length, pitch, and thickness of the adsorbent tube as optimization parameters. According to the results, the cylindro-conical receiver indicated the maximum optical efficiency of 85.42 %, the thermal efficiency of 67.95 %, and the maximum exergy efficiency of 35.73 %. They also introduced the conical geometry as the one with the best performance and the least performance for the cubical geometry. Soltani et al. [26] performed an experimental and numerical study of a cylindrical cavity receiver by developing a thermo-optical model. In this study, the effects of environmental parameters, the focal length of the concentrator, and variations in temperature and flow rate of the HTF on the thermal performance of the receiver were evaluated. They concluded that the operation of the receiver under optimal conditions increased the thermal efficiency up to 65 %. Thirunavukkarasu and Cheralathan [27] conducted an experimental study on a flat spiral tube receiver employed in a PDC. This study was conducted in different radiation conditions and for different temperature and flowrate values of the HTF. From the results, the energy and exergy efficiencies of the receiver were calculated as 56.21 % and 5.45 % at the average direct radiation of 750 W/m^2, respectively. Wang et al. [28] conducted an experimental and numerical study of three different geometries of the cavity receiver used in a food-grade Fresnel lens system. In this study, to increase the optical efficiency and better distribution of radiant flux in three cylindrical, spherical, and conical geometries, a metal cone reflector was used at the end of all three cavity holes. This metal cone reflector eventually caused a less than 2 % and 4 % increase in the optical efficiency of conical and spherical receivers, respectively.

Al-Dulaimi [29] conducted an experimental study of a flat-tube receiver with two layers of the absorbent tube employed in a PDC. The results indicated that the energy and exergy efficiencies of the system were 78.8 % and 19.8 %, respectively. Loni et al. [30] conducted an experimental and numerical comparative study among three hemispherical, cylindrical, and cubical cavity receivers. They also reviewed different types of cavity receivers used in PDCs. They used three types of nanomaterials based on thermal oil as HTFs. The results indicated that the use of nanomaterials in HTFs increased the thermal efficiency of each type of cavity receiver. Also, approximately 12.9 %, 5.84 %, and 1.44 % increases in efficiency were observed for hemispherical, cubical, and cylindrical receivers, respectively.

According to the literature, it was observed that several experimental and numerical studies were conducted on the optimization of geometry, increasing the values of energy and exergy efficiency and reducing the optical and thermal losses of cavity receivers. However, the employment of a conical cavity receiver in a PDC using thermal oil as the HTF was not experimentally investigated. Also, the thermal performance of the receiver with and without ultra-white glass cover on the aperture was experimentally and numerically investigated and profoundly discussed. The results of the current study could be used as a guide for the improvement of PDCs employed in different solar thermal applications using conical cavity receivers.

2. MATERIAL AND METHODS

2.1. Experimental setup

The experimental tests were conducted at the Renewable Energy Research Institute (RERI) of Tarbiat Modares University (TMU) located in Tehran (at 35.44° N latitude and 51.10° longitude), Iran. The developed solar collector in this

study consists of the main structure, a parabolic dish reflector, a conical cavity receiver, a hydraulic circuit, and a tracker system. The PDC is made of small pieces of mirrors (4 cm × 4 cm) sticking to a parabolic dish made of fiberglass. The dimensional characteristics of the reflector are presented in Table 1.

Table 1. Geometric parameters of the PDC used in the current study [7]

Parameter	Value
Aperture diameter	1.9 m
Focal length	1.35 m
Rim angle	36°
Reflectivity	0.84
Tracking error	1°
Concentration ratio	184

The conical cavity receiver was constructed according to the optimal dimensions reported in Refs. [31] and [32]. The preparation of the conical receiver was performed in four steps. First, the copper tube as an absorber tube was made in the form of springy and helical to create a conical shape. The cone angle of the receiver was chosen according to the geometry reported in Ref. [32]. The surface of the copper tube was coated with carbon black and matte refractory black paint (Ambrosol brand) to increase the absorptivity and reduce the reflectivity of the inner wall of the cavity. In the next step, the outer surface of the conical cavity receiver was completely covered with rock wool thermal insulation to minimize heat losses. Finally, the aperture of the receiver was covered with ultra-white glass to separate the inside and outside spaces of the cavity and reduce convective losses from the aperture of the receiver. The geometric characteristics of the conical receiver are presented in Table 2. Also, the images of the experimental setup along with the main components are shown in Figure 1a.

Table 2. Specifications of the cavity receiver

Parameter	Data
Cavity aperture's diameter (D_{ap})	14 cm
Diameter of the receiver (D_{ca})	18 cm
Length of the receiver (l)	14 cm
Outer diameter of the absorber tube (D)	11 mm
Inner diameter of the absorber tube (D_i)	9 mm
Pitch of the spiral coil	12 mm
Cone angle of the receiver (θ)	40°

The optical and thermal characteristics of the glass cover, properties of the refractory paint layer, and thermal properties of the used insulation are also presented in Table 3. All steps required for fabricating and preparing the receiver are presented in Figure 1b. A hydraulic circuit was installed on the system according to ASHRAE 93-86 standard (Ref. [33]). The main components of the hydraulic circuit are a 20-liter storage tank, a circulating pump, heat exchangers, and a conical receiver (as shown in Figure 2a). The HTF stored in the tank is circulated using a pump and its temperature rises by passing through the path 1-2-3. Then, it goes through heat exchangers by passing through the path 3-4. In this way, the heat absorbed by the HTF in the receiver is transferred to the cooling water and then, it returns to the oil storage tank.

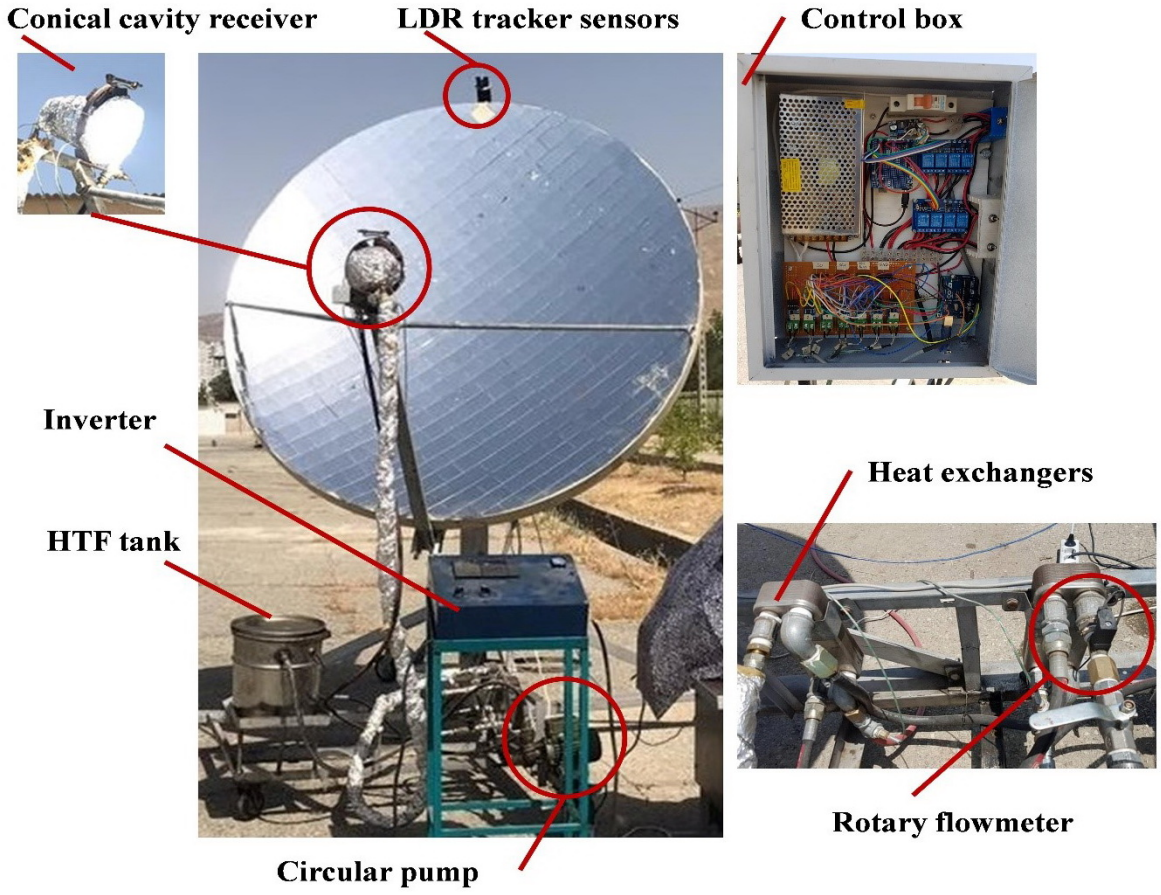

(a)

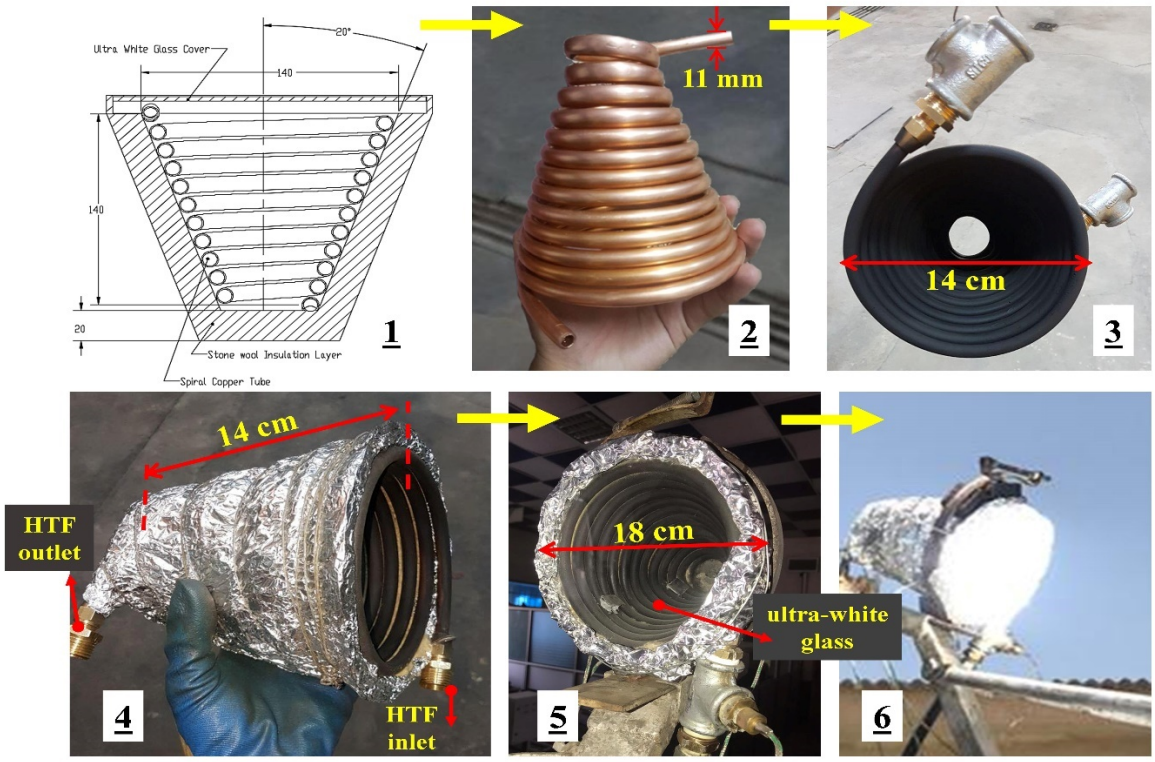

(b)

Figure 1. a) Photo of the experimental device and its main components, b) Different steps of fabricating the conical cavity receiver

Table 3. Properties of the materials used to construct the cavity receiver

Materials	Properties	Reason for use
Copper tube	• Thermal conductivity: 386 W/m.K • High melting point: 1000 °C [34]	Low thermal resistance
Black refractory coating	• Emissivity: 0.95 • Absorptivity: 0.9 • Stability: up to 700 °C	High absorptivity
Mineral wool insulation	• Thickness: 2 cm • Conductivity: 0.062 W/m.K [35]	Low thermal conductivity
Ultra-white glass cover	• Refractive index: 1.52 • Emissivity: 0.9	Low refraction

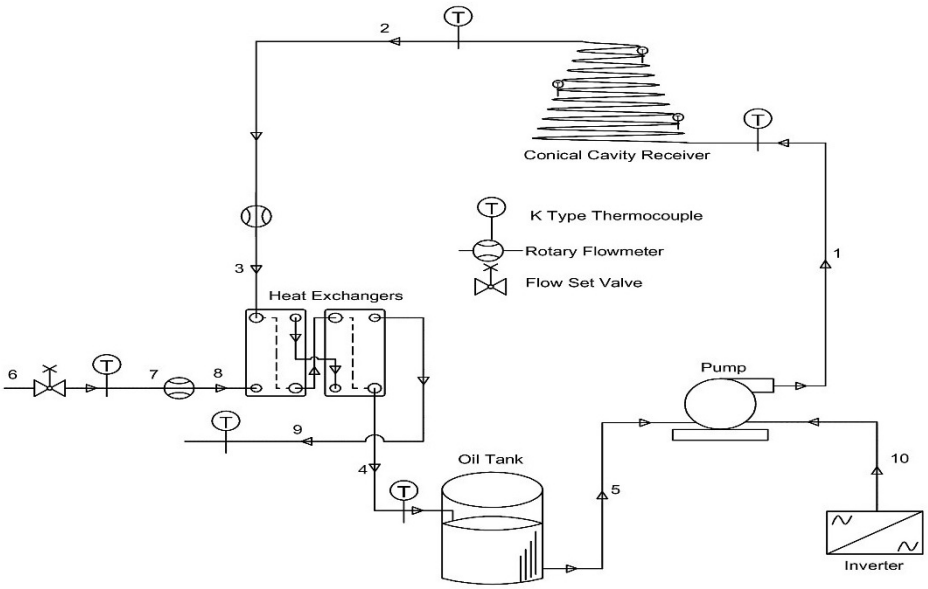

(a)

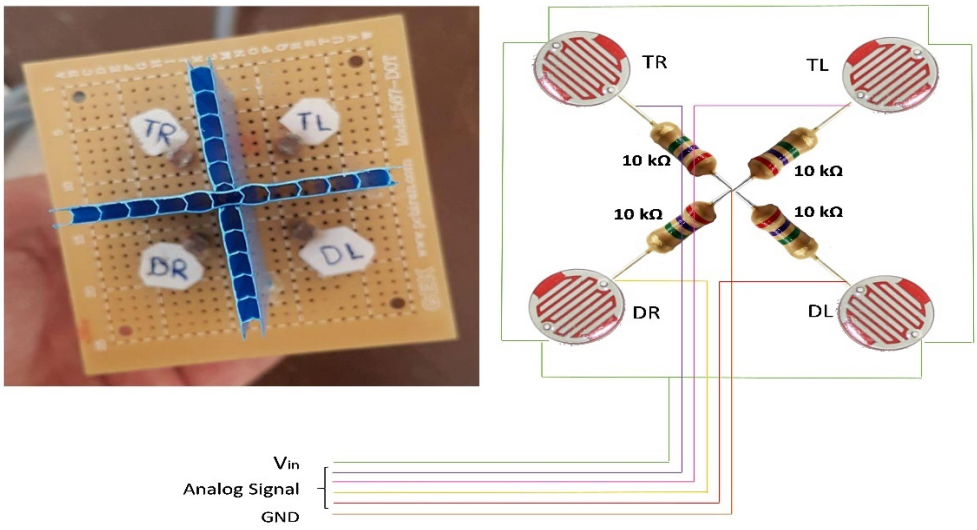

(b)

Figure 2. a) Schematic of the hydraulic circuit of the parabolic dish collector; b) The installation pattern of LDRs used to track the sun

In this study, a two-axis sun tracker composed of Light-Dependent Resistors (LDRs) was installed on the PDC system. The electronic circuit of the LDRs is presented in Figure 2b. The LDRs were installed on the upper part of the PDC and perpendicular to the reflector's surface. Due to variations in the angle of received solar radiation during the day, the internal resistance of LDRs related to each other varied and a signal was sent to the microcontroller such that the sun's path was processed and routed according to the defined algorithm of the microcontroller.

2.2. Uncertainty analysis

The measured parameters during the experiments were temperature, the HTF's volumetric flow rate, the amount of received solar radiation, wind speed, and air temperature. According to Figure 2a, the HTF's temperature at different locations including the inlet and outlet of the receiver and the exit of heat exchangers and the entrance of the tank, the temperature of the cooling water before and after entering the heat exchangers, and the temperature of the inner wall of the receiver were measured. Additionally, the volumetric flow rates of the HTF and cooling water (as shown in Figure 2a) were measured using turbine rotary flowmeters (Vision; type 2000). Also, K-type thermocouples (Chromel-Alumel) were employed to measure the temperature of different parts of the system. The data were then collected in a data logger for further analysis. The solar radiation was measured using the TES-1333 solar power meter and the wind speed was measured using the CT-AM 4220 anemometer. The calibration of K-type thermocouples and data logger was performed using TES-1307 thermometers along with a glass of ice and boiling water. Also, the flowmeters were calibrated by pouring water inside a scaled cylinder during a specific period. In this study, thermal efficiency uncertainty was calculated as 1.18 % using Eq. 1. [21]:

$$\frac{U\eta_{th}}{\eta_{th}}=\sqrt{\left(\frac{U\dot{Q}_{solar}}{\dot{Q}_{solar}}\right)^2+\left(\frac{U\Delta T}{\Delta T}\right)^2+\left(\frac{U\dot{m}}{\dot{m}}\right)^2} \quad (1)$$

The accuracy values for measuring instruments along with uncertainty values are presented in Table 4. Since only the measured temperature of the HTF is affected by other measured parameters, the standard uncertainty analysis of the HTF's temperature was performed using the Guide for Expression of Uncertainty in Measurement (GUM) method, as presented in Ref. [36]:

$$u=\sqrt{\frac{\sum_{i=1}^{n}(X_i-\bar{X})^2}{n(n-1)}} \quad (2)$$

where X and $\bar{X}$ are the measured and average temperature values of the HTF, respectively, n is the sample count, and u is the standard uncertainty. Using this formula, the maximum values of the standard uncertainty were calculated as 0.365 and 0.666 for the conical cavity receiver with and without a glass cover on the aperture, respectively.

Table 4. Accuracy values and ranges for measuring instruments

Instrument type	Resolution	Accuracy	Range of operation	Uncertainty (%)
K-type thermocouples	0.25 °C	± 0.56 °C	0-1000 °C	0.26
Solar power meter	0.1 W/m^2	± 0.11 W/m^2	0-2000 W/m^2	0.26
Anemometer	0.1 m/s	± 0.2 m/s	0.9-35 m/s	10
Rotary flowmeter	0.01 mA	± 0.05 mA	0-20 mA	

3. NUMERICAL INVESTIGATION

3.1. Boundary conditions

In this study, only the thermal model of the conical cavity receiver was evaluated. Boundary conditions and experimental test conditions for the numerical solution are negligible heat loss from the outer surface of the insulation, constant temperature of the oil tank, the HTF's temperature of 50 °C at the entrance of the receiver, equal pressure of separate air between the cavity and the glass cover with the

ambient air, oil pressure equal to ambient pressure due to the open circuit of the hydraulic cycle, and the constant oil flow rate of 0.7 l/min in the circuit.

3.2. Heat transfer analysis

The amount of heat loss from the cavity receiver depends on various factors such as the geometry of the concentrator and receiver, temperatures of the HTF at the inlet and outlet of the receiver, temperature of the inner wall of the cavity, ambient temperature, emissivity of the inner surface and glass cover of the cavity, etc. The schematic of the heat transfer model governing the receiver in this study is shown in Figure 3.

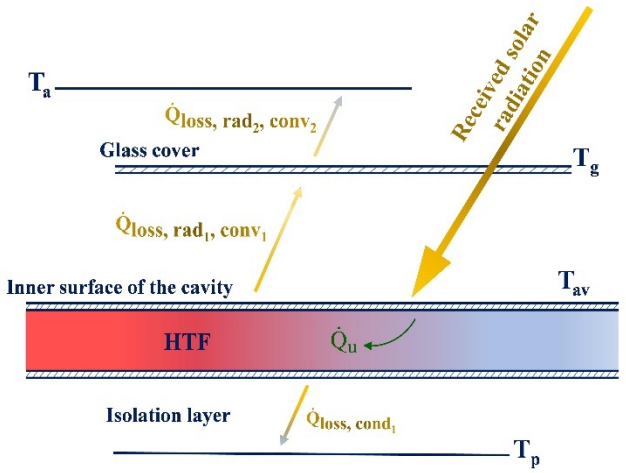

Figure 3. The schematic of the heat transfer model governing the receiver with ultra-white glass cover

The net heat transfer rate of the absorber tube was calculated as [34]:

$$\dot{Q}_u = \dot{Q}^* - \dot{Q}_{loss} \quad (3)$$

$$\dot{Q}_{loss} = \dot{Q}_{loss,cd} + \dot{Q}_{loss,cv} + \dot{Q}_{loss,r} \quad (4)$$

$$\dot{Q}^* = \eta_{optical} A_{ref} \dot{Q}_{solar} \quad (5)$$

According to Eq. 3, the rate of useful energy absorbed by the receiver is obtained by subtracting the heat loss rate from the amount of solar radiation received by the receiver ($\dot{Q}^*$). The receiver's total heat loss occurs through the main heat transfer mechanisms of conduction ($\dot{Q}_{loss,cd}$), convection ($\dot{Q}_{loss,cv}$), and radiation ($\dot{Q}_{loss,r}$), as presented in Eq. 4. Under the steady-state conditions, heat loss from the cavity receiver occurs when the aperture is covered with an ultra-white glass which can be calculated as follows [33]:

$$\dot{Q}_{loss} = \dot{Q}_{loss,\ cd1} + \dot{Q}_{loss,cv1} + \dot{Q}_{loss,r1} = \dot{Q}_{loss,cv2} + \dot{Q}_{loss,r2} \quad (6)$$

According to this equation, the rate of heat loss is equal to the losses that occur between the walls of the receiver and the inner surface of the glass cover, as well as the outer surface of the glass cover and the ambient. Herein, $\dot{Q}_{loss,\ cd1}$, $\dot{Q}_{loss,cv1}$, $\dot{Q}_{loss,r1}$, $\dot{Q}_{loss,cv2}$, and $\dot{Q}_{loss,r2}$ are the rates of conduction losses between the surface of the receiver and the glass cover, convection losses between the inner wall of the cavity and the glass cover, radiation losses between the inside walls of the cavity and the glass cover, convection losses from the outer surface of the glass cover to the ambient, and radiation losses from the outer surface of the glass cover to the air, respectively. The rates of heat loss from the inner wall of the receiver to the glass cover are calculated as follows [33]:

$$\dot{Q}_{loss,cd1} = \frac{\pi l \lambda (T_{av} - T_p)}{\ln(r_2/r_1)} \quad (7)$$

$$\dot{Q}_{loss,cv1} + \dot{Q}_{loss,rd1} = \pi r_1 l (h_{cv1} + h_{r1})(T_{av} - T_g) \quad (8)$$

where l, λ, r_2, r_1, T_{av}, T_p, and T_g are the effective length of the cavity receiver, the thermal conductivity of the insulation material, the radius of the cavity and the insulation layer, the average temperature of the inner wall of the cavity, the surface temperature of the insulation, and the temperature of the glass cover, respectively. h_{cv1} and h_{r1} are coefficients of convective and radiative heat losses and are calculated as follows [37]:

$$h_{cv1} = \frac{0.212 \lambda (Gr_\delta\ p_r)^{1/4}}{\delta} \quad (9)$$

$$h_{r1} = \frac{\sigma (T_{av}^2 + T_g^2)(T_{av} + T_g)}{\frac{1}{\varepsilon_{av}} + \frac{A_{av}}{A_g}\frac{1}{\varepsilon_g} - 1} \quad (10)$$

where δ is the average space between the inner wall of the cavity and the glass cover, Gr is the Grashof number, P_r is the Prandtl number, σ is the Stefan Boltzmann constant, and ε_{av} and ε_g are the inner wall emissivity of the cavity and the emissivity of the glass cover, respectively. A_{av} and A_g are the inner surfaces of the cavity and glass cover, respectively. Considering Eqs. 11 and 12, the rate and the overall coefficient of heat loss from the cavity are calculated as follows:

$$\dot{Q}_l = A_{av} U_l (T_{av} - T_a) \quad (11)$$

$$U_l = \frac{\frac{\lambda (T_{av} - T_p)}{r_1 \ln(r_2/r_1)} + \frac{0.212 \lambda (Gr_\delta\ p_r)^{1/4}}{\delta}(T_{av} - T_g) + \frac{\sigma (T_{av}^2 + T_g^2)(T_{av} + T_g)}{\frac{1}{\varepsilon_{av}} + \frac{A_{av}}{A_g}\frac{1}{\varepsilon_g} - 1}(T_{av} - T_g)}{T_{av} - T_a} \quad (12)$$

According to the rate of heat loss calculated by Eq. 11, the rate of useful gained heat considering the overall coefficient of heat loss from the receiver is calculated as follows:

$$\dot{Q}_u = A_r [S - U_l'(T_{av} - T_a)] \quad (13)$$

$$S = \eta_{optical} I C \sin\frac{\theta}{2} \quad (14)$$

$$U_l' = U_l C \sin\frac{\theta}{2} \quad (15)$$

where A_r, T_a, I, C, and θ are the cavity's aperture area, ambient temperature, received solar radiation, the geometrical concentration ratio of the concentrator, and conical receiver's cone angle, respectively. The useful gained energy which is transferred to the HTF can be calculated from Eq. 16:

$$\dot{Q}_u = \frac{L(T_{av} - T_i)}{\frac{1}{\pi D_i h_{fi}} + \frac{1}{2\pi\lambda}\ln\frac{D}{D_i}} \quad (16)$$

$$L = \frac{\pi w (D + w)}{4D \sin(\frac{\theta}{2})} \quad (17)$$

where T_i is the temperature of the HTF at the inlet of the cavity, D and D_i are outer and inner diameters of the absorber

tube, respectively, h_{fi} is the convective heat transfer coefficient of the HTF at the inlet of the receiver, and w and L are the aperture diameter of the cavity and the total length of the absorber tube, respectively. The rate of useful energy absorbed by the HTF can be obtained through Eq. 18 [33]:

$$\dot{Q}_u = A_r F_R C \sin\frac{\theta}{2}[\eta_{optical} I - U_l(T_i - T_a)] \quad (18)$$

$$F_R = \frac{4\dot{m}C_p}{\pi w^2 U_l C \sin\frac{\theta}{2}}\{1 - \exp[-\frac{\pi w^2 (D + w) U_l F'}{4D \sin\frac{\theta}{2}\dot{m}C_p}]\} \quad (19)$$

$$F' = \frac{1/w}{\frac{4}{C\pi w^2 \sin\frac{\theta}{2}} + \frac{4D\sin\frac{\theta}{2}}{\pi w(D+w)}(\frac{1}{\pi D_i h_{fi}} + \frac{1}{2\pi\lambda}\ln\frac{D}{D_i})U_l} \quad (20)$$

where F_R and F' are heat removal and efficiency factors of the collector, respectively. Also, the overall heat loss coefficient of the cavity receiver (U_l) without the glass cover on the aperture can be calculated as follows [38]:

$$U_l = \frac{Nu\, k}{D_{ap}} + \frac{\sigma(T_{av}^2 + T_a^2)(T_{av} + T_a)}{1 + (\frac{1-\varepsilon}{\varepsilon})\frac{A_{ap}}{A_{av}}} \quad (21)$$

$$Nu = 1.635\, Re^{0.38} Pr^{-1.2} (\frac{D_{ap}}{D_{ca}})^{0.892} (1 + \cos\emptyset)^{0.285} \quad (22)$$

In Eq. 21, U_l consists of the convection and radiative heat transfer coefficients, Nu is the non-dimensional Nusselt number of the wind flow near the receiver aperture which was experimentally calculated using Ref. [39] and used in Ref. [40] to validate the simulation and a correlation of over 83 %, k is the air's thermal conductivity, and D_{ap} is the diameter of the cavity's aperture. The Nu is calculated from Eq. 22, where $\emptyset$ is the inclination angle of the receiver. The thermal efficiency of PDCs can be calculated as follows [33]:

$$\eta_{th} = \frac{\dot{Q}_u}{\dot{Q}^*} = \frac{\dot{Q}^* - \dot{Q}_{loss}}{\eta_{optical} A_{ref} \dot{Q}_{solar}} \quad (23)$$

$$\eta_{opt} = \frac{\dot{Q}^*}{A_{ref}\dot{Q}_{solar}} \quad (24)$$

The thermal model of the cavity receiver with the aperture covered with a glass cover was solved by Newton-Raphson root-finding method in Fortran software with four equations and four unknowns. Using this method, four unknown temperature values of the ultra-white glass cover, the temperature of the cavity's inner wall, the rate of the useful gained heat ($\dot{Q}_u$) by the receiver and the HTF, and the rate of the heat loss ($\dot{Q}_{loss}$) from the receiver were obtained. Also, considering the cavity without the glass cover, two equations and two unknowns were solved. Finally, the two unknown temperature values of the inner wall of the cavity receiver and the rate of gained useful energy ($\dot{Q}_u$) were obtained.

4. RESULTS AND DISCUSSION

Experimental tests were performed continuously from 10:00 to 16:00. During the tests, the viscosity of the HTF varied by temperature variations. Therefore, to keep the volumetric flow rate of the oil constant, an inverter was used to control the speed of the oil pump (shown in Figure 1a). During the tests, the temperature of the oil before entering the receiver (temperature of the stored oil in the tank) was kept constant by continuously monitoring the HTF's temperature and variations in the flow rate of the cooling water flowing in heat exchangers.

4.1. Experimental results

4.1.1. Conical cavity receiver with ultra-white glass on the aperture

The conical cavity receiver of the PDC with an ultra-white glass cover on its aperture was evaluated on 4th July 2020 under climate conditions of Tehran, Iran. Figure 4a shows the variations in solar radiation and the air temperature, as well as the temperature difference between the HTF at the inlet and outlet of the receiver. During the test, the oil temperature at the inlet of the receiver was kept constant at 50 °C and its flow rate at 0.7 l/min. According to Figure 4a, the maximum amount of radiation was recorded as 965.6 W/m^2 at 13:00 and the minimum value was recorded as 917.8 W/m^2 at 10:00 (in the morning). As shown in this figure, differences in the temperature of the oil at the inlet and outlet of the receiver follow the same trend of variations in solar radiation with the maximum difference of 69 °C at 13:00 and the minimum difference of 63.25 °C at 10:00. Also, the air temperature in the middle of the day was recorded as 33 °C, which was higher than the initial and final hours with the recorded temperature value of 29 °C at 16:00.

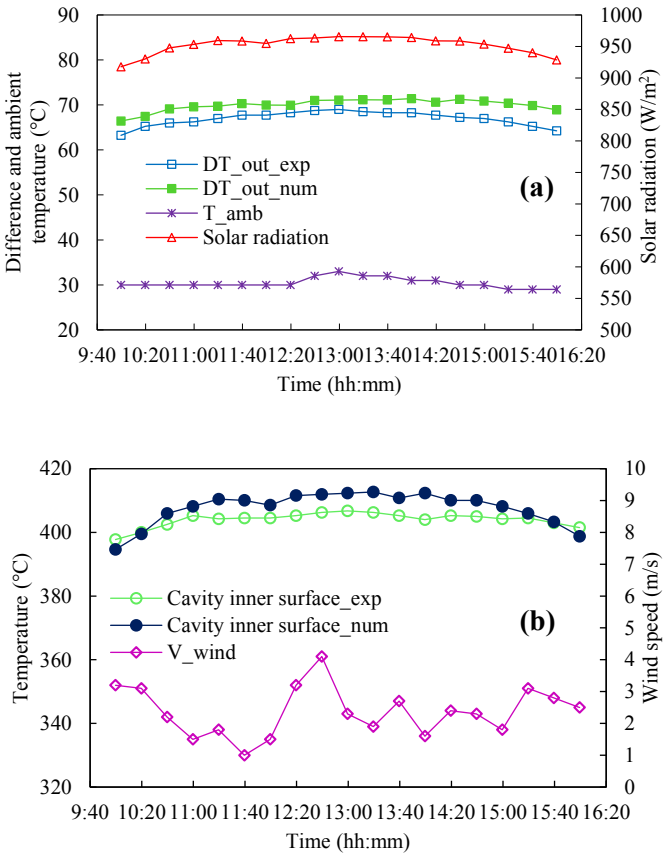

Figure 4. a) Variations of different environmental and operational parameters (on 4th July), b) Variations in the temperature of the inner wall of the receiver and wind speed (on 4th July)

The variations in the temperature of the inner wall of the receiver and the wind speed are shown in Figure 4b. According to this figure, it can be seen that the highest surface

temperature is 406.75 °C between 12:40 and 13:20. It can also be seen that the variation in the receiver's wall temperature approximately follows the trend of the solar radiation variation. This figure shows variations in the wind speed during the evaluation day, ranging from 1 m/s at 11:40 to 4.1 m/s at 12:40. According to the figure, it appears that due to the existence of the glass cover on the receiver aperture, variations in wind speed could not significantly affect the receiver's surface temperature.

The rate of heat absorbed by the HTF inside the receiver and also thermal efficiency of the receiver are shown in Figure 5. The figure shows that at 13:00, the maximum heat of 1,291.68 W was absorbed by the receiver, while the minimum values were recorded at 10:00 and 16:00 (initial and final hours of the evaluation day) as 1,184.04 W and 1,202.76 W, respectively. Also, the highest thermal efficiency of the PDC was reported as 53.51 % at 13:00. According to the numerical analyses, it was found that by increasing the temperature of the HTF at the inlet of the receiver, the temperature of the HTF at the outlet of the receiver and the temperature of the inner wall of the receiver increased, while the useful absorbed heat and the thermal efficiency of the system decreased. Similar results have been reported in Refs. [21] and [41].

4.1.2. Conical cavity receiver without ultra-white glass on its aperture

Experimental evaluations of the PDC collector with a conical cavity receiver without a glass cover on the aperture were performed on 7th July 2020. The evaluations were performed similarly to the experiments performed for the receiver with a glass cover. The flow rate and temperature of the HTF at the inlet of the receiver were constant at 0.7 l/min and 50 °C, respectively. According to Figure 6a, the solar radiation variation reaches the highest value of 967.5 W/m^2 at 13:00 and the lowest value of 935.9 W/m^2 at 10:00 on 7th July. Also, the highest temperature difference of the HTF at the inlet and outlet of the receiver was recorded as 56.25 °C from 12:40 to 13:20 with the air temperature variations in the range of 25-33 °C at 10:00 and 13:00, respectively.

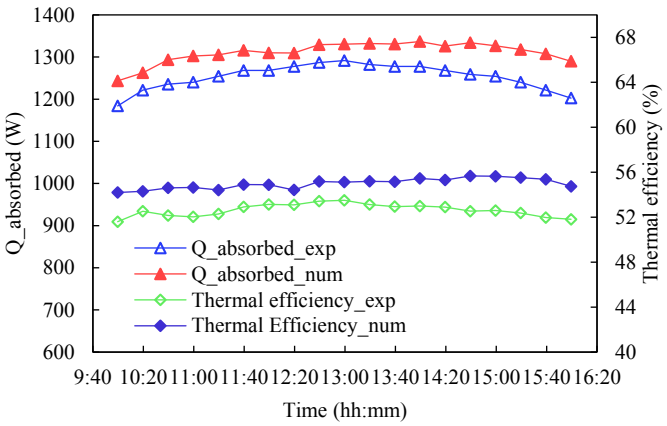

Figure 5. Variations in the absorbed energy and the thermal efficiency of the conical cavity receiver on 4th July

Figure 6b shows variations of the inner wall of the receiver and changes in the wind speed during experiment hours. The maximum temperature of the inner wall of the receiver was recorded as 382.5 °C at 13:20. According to this figure and considering that the aperture of the receiver is not covered (thus, it is exposed to the wind streams), a decline in the temperature of the inner surface of the receiver from its mean value of 377.3 °C in the previous hours (10:00 to 15:00) to 366.25 °C is observed at the final hours of the experiment. Likewise, the wind speed increased from its mean value of 2.6 m/s at the previous hours (10:00 to 15:00) to 5.3 m/s, while at the hour between 10:00-15:00, the wind speed showed steady fluctuations.

Figure 7 shows the variations in the amount of useful absorbed energy and the thermal efficiency of the system during evaluation hours. It can be seen that the most useful heat of 1,053 W was absorbed between 12:40-13:20. Also, the highest thermal efficiency ranging from 42.66 % to 43.03 % was recorded during the same period. It can be observed that the curves of the useful absorbed heat and thermal efficiency follow a similar trend of the temperature difference of the HTF at the inlet and outlet of the receiver.

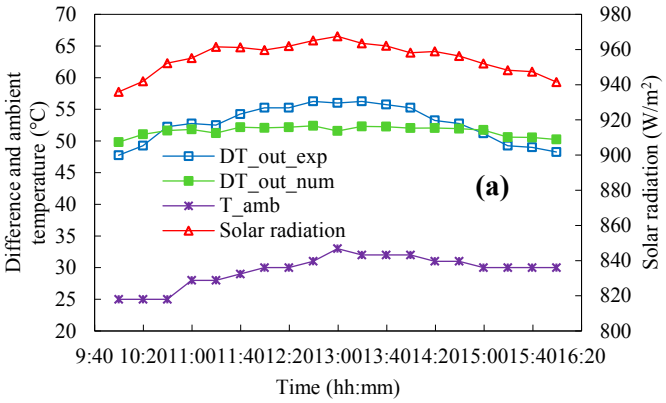

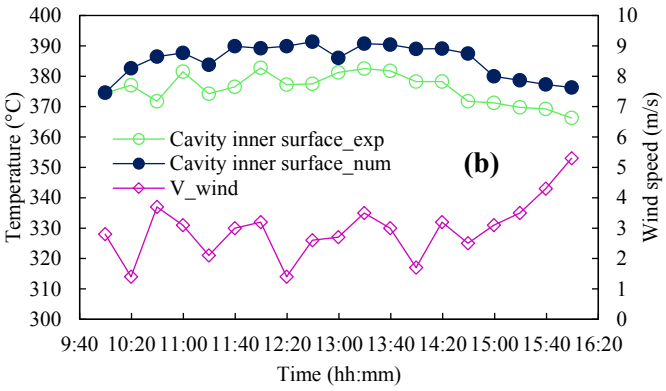

Figure 6. a) Variations of different parameters of the conical cavity receiver; b) Variations in the temperature of the cavity inner surface and wind speed on 7th July

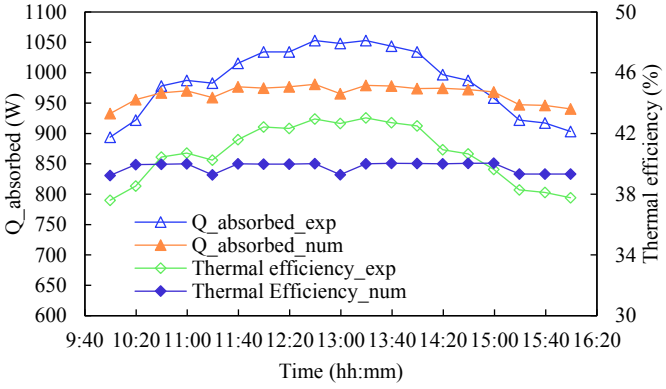

Figure 7. Variations in the absorbed energy and the thermal efficiency of the receiver on 7th July

4.2. Numerical modeling results and validation

In the numerical study, by solving the governing equations of the PDC and the receiver using Fortran software, the parameters of HTF temperature at the outlet of the receiver, the temperature of the inner wall of the receiver, and also the rate of the useful absorbed heat were calculated. Also, the value of the thermodynamic efficiency of the system was obtained. The results of the numerical simulation of the receiver with the aperture covered with an ultra-white glass and the aperture with no glass cover are presented in Figures 4 to 7.

The results of the numerical simulations do not differ much from the results of experimental tests. The reason could be the proper definition of the environmental, geometric, optical, and thermal parameters of the cavity receiver. Table 5 reports the values of the measured parameters including the temperature of the HTF at the inlet of the receiver, solar radiation, air temperature, and wind speed on 4th and 7th July. Also, according to Tables 6 and 7, it can be seen that in the case of the receiver with the glass cover, there are 2.05 %, 1.46 % and 3.56 % differences for the experimental and numerical data of the temperature of the HTF at the inlet and outlet of the receiver, the temperature of the inner wall of the receiver, and thermal efficiency, respectively. In the case of the receiver without a glass cover, the differences between numerical and experimental values of the mentioned parameters are 3.40 %, 2.45 % and 6.45 %, respectively.

Table 5. Measured parameters at the steady-state test times on 4th and 7th July

Time	Measured parameters on 4th July 2020				Measured parameters on 7th July 2020			
	T_{in} (°C)	I_{solar} (W/m^2)	T_{amb} (°C)	V_{wind} (m/s)	T_{in} (°C)	I_{solar} (W/m^2)	T_{amb} (°C)	V_{wind} (m/s)
11:40	-	-	-	-	50.50	961.2	29	3.0
12:00	50.25	959.7	30	1.5	50.25	959.7	30	3.2
12:20	51.00	961.9	30	3.2	49.75	961.9	30	1.4
12:40	49.75	965.1	31	4.1	50.25	965.1	31	2.6
13:00	49.5	967.5	33	2.3	50.00	967.5	33	2.7
13:20	50.00	963.5	32	1.9	50.50	963.5	32	3.5
13:40	50.25	962.1	32	2.7	49.75	962.1	32	3.0
14:00	50.00	958.2	32	1.6	50.25	958.2	32	1.7

Table 6. Comparison between experimental and numerical results for the receiver with an ultra-white glass cover on 4th July

Time	Experimental				Numerical				Derivation		
	T_{out} (°C)	T_{surf} (°C)	Q_{abs} (W)	η_{th} (%)	T_{out} (°C)	T_{surf} (°C)	Q_{abs} (W)	η_{th} (%)	D_{Tout} (%)	D_{Tsurf} (%)	$D_{\eta th}$ (%)
11:40	117.75	404.50	1268.28	52.92	120.29	410.06	1315	54.90	2.16	1.38	3.75
12:00	117.75	404.50	1268.28	53.14	119.98	408.5	1310	54.89	1.89	1.00	3.29
12:20	118.25	405.25	1277.64	53.10	119.96	411.5	1309	54.43	1.44	1.56	2.50
12:40	118.75	406.25	1287.00	53.43	121.01	411.9	1329	55.18	1.90	1.40	3.28
13:00	119.00	406.75	1291.68	53.51	121.09	412.3	1330	55.20	1.75	1.37	3.02
13:20	118.50	406.25	1382.32	53.13	121.16	412.7	1332	55.20	2.25	1.59	3.89
13:40	118.25	405.25	1277.64	52.95	121.10	410.8	1330	55.46	2.41	1.37	4.17
14:00	118.25	404.00	1277.64	52.99	121.41	412.3	1336	55.45	2.67	2.06	4.63

Table 7. Comparison between experimental and numerical results for the receiver without cover on 7th July

Time	Experimental				Numerical				Derivation		
	T_{out} (°C)	T_{surf} (°C)	Q_{abs} (W)	η_{th} (%)	T_{out} (°C)	T_{surf} (°C)	Q_{abs} (W)	η_{th} (%)	D_{Tout} (%)	D_{Tsurf} (%)	$D_{\eta th}$ (%)
12:00	105.25	382.75	1034.28	42.43	102.07	389.20	974.7	39.99	3.02	1.69	5.76
12:20	105.25	377.25	1034.28	42.33	102.18	389.90	976.7	39.98	2.95	3.35	5.56
12:40	106.25	377.50	1053.00	42.96	102.40	391.36	980.9	40.02	3.62	3.67	6.84
13:00	106.00	381.25	1048.32	42.66	101.58	386.01	965.5	39.29	4.17	1.25	7.89
13:20	106.25	382.50	1053.00	43.03	102.30	390.72	979.0	40.01	3.72	2.15	7.02
13:40	105.75	381.75	1043.64	42.71	102.26	390.42	978.2	40.03	3.30	2.27	6.27
14:00	105.25	378.25	1034.28	42.50	102.03	388.96	974.0	40.02	3.06	2.83	5.82

4.3. Comparison of performances

The thermal performance of a PDC with a conical cavity receiver with and without ultra-white glass cover on its aperture was numerically and experimentally investigated on 4th and 7th July 2020 with similar environmental conditions. Table 8 shows the mean values of solar radiation, air temperature, and wind speed with the measured values already reported in Table 5 for the same evaluation days. Observing average values of mentioned parameters shows similar amounts of these values for each day of the experiment. Also, the volume flow rate and the HTF's temperature at the inlet of the receiver were the same in both cases.

Figure 8a shows the experimental values of the HTF's temperature at the outlet of the receiver and the temperature of the inner wall of the cavity, while Figure 8b shows the

experimental values of the useful gained heat by the HTF and the thermal efficiency of the receiver with and without a glass cover on its aperture. Furthermore, Table 9 shows the maximum, minimum, and mean values of the mentioned parameters.

Table 8. Comparison between the mean values of measured parameters on 4th and 7th July

Conical cavity receiver	$I_{solar\text{-}ave}$ (W/m²)	$T_{amb\text{-}ave}$ (°C)	$V_{wind\text{-}ave}$ (m/s)
With glass cover (4th July 2020)	953.33	30.27	2.34
Without glass cover (7th July 2020)	955.26	29.57	2.95

Upon comparing the mean values of the parameters presented in Table 9, it is observed that by installing the glass cover on the receiver aperture, the HTF's temperature at the outlet of the receiver and the temperature of the inner wall of the receiver increase to 14.19 °C and 28.04 °C, respectively. Also, the increase of 11.94 % in the thermal efficiency of the receiver was observed. Similar results were reported in the numerical results reported in Ref. [18] with a 7 % increase in thermal efficiency in the case of the glass cover on the receiver aperture. Figure 9 shows the overall efficiency of the receiver versus the value of $(\frac{T_i - T_a}{I_b})$ with and without a glass cover on the receiver's aperture, respectively. Both diagrams presented in Figure 9 are plotted at the time interval when the system is in the steady state (the time interval is shown in Figure 8b). For the cavity with and without a glass cover, the predicted models according to the experimental results are described as:

$$\eta_{th} = 0.5581 - 1.4178(\frac{T_i - T_a}{I_b}) \quad (25)$$

$$\eta_{th} = 0.4411 - 0.755(\frac{T_i - T_a}{I_b}) \quad (26)$$

Based on Figure 9 and considering Eqs. 25 and 26, it is found that the slope and coordinate distance constant of the plotted graphs are equal to $\frac{F_R U_l}{C}$ and $F_R\eta_{opt}$, respectively.

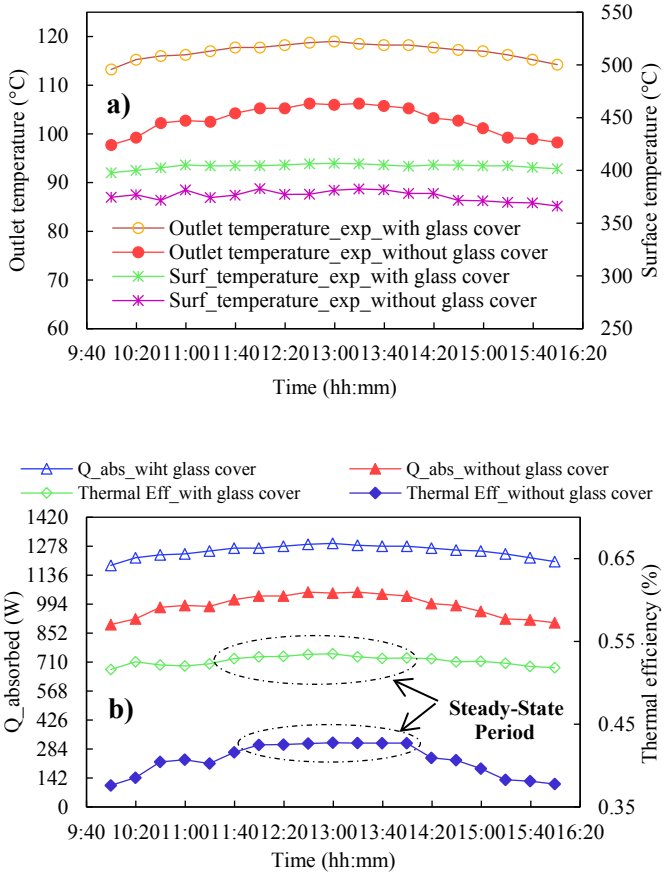

Figure 8. a) Temperature of the HTF at the outlet of the receiver and the temperature of the cavity's inner wall based on experimental results; b) Heat gained by the HTF and the receiver's thermal efficiency based on experimental results

Table 9. Comparison between the results for the conical cavity receiver with and without an ultra-white glass cover on its aperture based on experimental results

Conical cavity receiver	$T_{out\text{-}max}$ (°C)	$T_{out\text{-}min}$ (°C)	$T_{surf\text{-}max}$ (°C)	$T_{surf\text{-}min}$ (°C)	$Q_{abs\text{-}max}$ (w)	$Q_{abs\text{-}min}$ (w)	$\eta_{th\text{-}max}$ (%)	$\eta_{th\text{-}min}$ (%)
With ultra-white glass cover	119	113.2	406.75	397.75	1291.1	1184.4	53.51	51.60
Average values	116.95		404		1253.25		52.63	
Without ultra-white glass cover	106.25	97.75	382.75	366.25	1053	893.88	42.75	37.60
Average values	102.76		375.96		987.68		40.69	

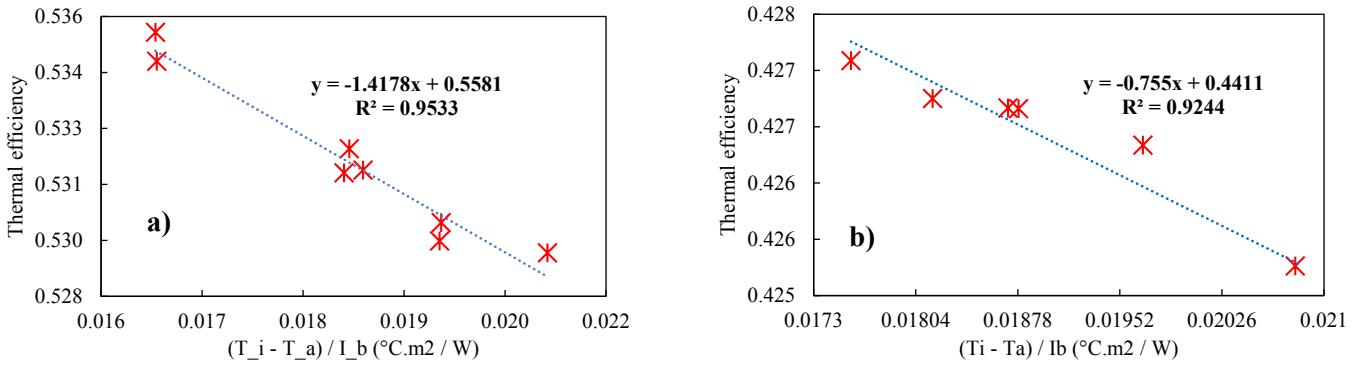

Figure 9. Overall thermal efficiency of the receiver versus $(\frac{T_i - T_a}{I_b})$ for the receiver: a) with the glass cover, b) without the glass cover

Table 10 shows the values of $F_R\eta_{opt}$, $\frac{F_R U_l}{C}$, F_R, U_l, and $\frac{U_l}{C}$. It can be found that the values of F_R (heat removal factor of the PDC) and U_l (overall heat loss coefficient) of the receiver with the glass cover are higher than those in the case without the glass cover. Upon comparing Eqs. 25 and 26 and considering the obtained results presented in Table 10, it is found that due to the higher efficiency achieved for the receiver with the glass cover, the higher temperature of the HTF at the outlet of the receiver, and the high value of the F_R for the conical cavity receiver, the value of U_l is less than that obtained for the receiver without the glass cover. Similar results were reported in Ref. [21] for two cylindrical and cubical cavity receivers, where a lower value of U_l and a larger value of F_R were obtained for the cubical receiver than those for the cylindrical type because of the higher performance of the cubical receiver. It should be mentioned that the optical efficiency of the parabolic concentrator was assumed as 90 % in all calculations.

It is concluded that for the conical cavity receiver with the glass cover on its aperture, by reaching high temperature values for the inner wall of the cavity, higher values of F_R and lower values of the overall heat loss from the receiver (U_l) are achievable for the receiver without the glass cover.

Table 10. Comparison between overall heat loss coefficient and heat removal factor of the PDC and the receiver with and without an ultra-white glass cover on the aperture

Conical cavity receiver	$F_R\eta_{opt}$	$\frac{F_R U_l}{C}$	F_R	C	U_l	$\frac{U_l}{C}$
With ultra-white glass cover	0.5581	1.4178	0.62	184	420.76	2.28
Without ultra-white glass cover	0.4411	0.755	0.49	184	283.51	1.54

Similar results for η_{opt} are reported in Ref. [33] for three conical, cubical, and cylindrical cavity receivers (with glass cover on their aperture) installed on a Fresnel lens system. Also, similar results for η_{th} were reported in Ref. [21] for two cubical and cylindrical cavity receivers used in a PDC. To calculate the divergence of the thermal efficiency of the conical cavity receivers with and without ultra-white glass cover, the Root-Mean-Square Error (RMSE) was used. Table 11 shows the estimated RSME values under the steady-state condition. The RMSE can be calculated as:

$$RMSE=\sqrt{\frac{\sum_{i=1}^{N}(\bar{Y}_i-Y_i)^2}{N}} \quad (27)$$

where N is the total number of the calculated parameters under the steady-state condition, Y_i is the calculated parameter, and $\bar{Y}_i$ is the average of the calculated parameter.

Table 11. Estimated RSME values for the thermal efficiency and heat gain of the cavity receiver

Conical cavity receiver	RMSE for cavity heat gain (W)	RMSE for thermal efficiency (%)
With glass cover	7.6722	0.57
Without glass cover	8.07	0.09

5. CONCLUSIONS

In this study, the thermal performance of a PDC employing a conical cavity receiver was numerically and experimentally investigated. The effect of the presence and absence of the ultra-white glass cover on the aperture of the receiver on the thermal performance of the PDC and receiver was investigated. In the experiments, environmental and operational parameters were measured, recorded, and analyzed. From this study, the following points are concluded:

- According to the experimental and numerical results, it was found that there was good agreement between the experimental and numerical results. For the receiver with glass cover on its aperture and without glass cover, 2.67 % and 3.06 % deviations in HTF's outlet temperature were observed. Also, 2.06 % and 2.83 % deviations in the cavity's inner surface temperature and 4.63 % and 5.82 % deviations in the useful heat gained by the HTF and thermal efficiency of the PDC were observed.
- It was found that by covering the aperture of the cavity, the average concentrating thermal efficiency increased from 11.92 % to 52.63 %.
- The useful heat absorbed by the HTF and the temperature of the HTF at the inlet of the receiver were obtained as 1253.25 W, 116.95 °C for the cavity with the glass cover and 987.68 W and 102.76 °C for the cavity without the glass cover.
- In the diagram representing thermal efficiency versus $\frac{T_i - T_a}{I_b}$, it was observed that due to the higher values of efficiency, the parameter F_R for the conical cavity receiver with the glass cover on its aperture was 0.62, being more than that of the cavity without the glass cover (0.49).
- The value of U_l for the receiver with the glass cover on its aperture was 420.76 W/m^2°C. The reason for its high value compared to the case of no glass cover on the aperture is the high value of the useful absorbed heat and the high temperature of the inner surface of the cavity, as well as the high amount of heat loss.

Considering that the present study is a thermal investigation of a CSP system and due to the appropriate thermal performance of the conical cavity receiver with the glass cover on its aperture, this system can be used as a study to build a PDC on a larger scale in a CSP power plant to generate electricity employing thermodynamics cycles. For further studies, it is also recommended that different types of nanofluids with the oil-based fluid used as the HTF in this study be compared, and also, steam generator power cycles working based on PDCs be studied.

6. ACKNOWLEDGEMENT

The authors would like to thank the advisory support received from the Renewable Energy Research Institute, an affiliation of Tarbiat Modares University (TMU) (http://www.modares.ac.ir) and the received financial support (grant number IG/39705) for the 'Renewable Energies Research Group'.

NOMENCLATURE

$\dot{Q}^*$	Rate of available solar heat for concentrator (W)
$\dot{Q}_u$	Net heat transfer rate (W)
$\dot{Q}_{loss}$	Thermal heat losses (W)
I	Solar radiation (W/m^2)
h	Convection heat transfer coefficient (W/m^2°C)
T	Temperature (°C)
r	Radiation (m)
l	Length (m)
L	Length of the absorber tube (m)
A	Area (m^2)
δ	Average space between cavity and glass cover (m)
U_l	Overall heat loss coefficient (W/m^2°C)
F_r	Collector heat removal factor
C	Concentration ratio
u	Uncertainty
n	Sample count
$\eta_{optical}$	Optical efficiency (%)
η_{th}	Thermal efficiency (%)
$\bar{X}$	Average value of the measured HTF temperature (°C)
X	Measured HTF's temperature (°C)
Pr	Prandtl number
Gr	Grashof number
Nu	Nusselt number
Greek letters	
ε	Emissivity
λ	Thermal conductivity (W/m. K)
θ	Cone angle of the receiver (°)
Ø	Inclination angle of the receiver (°)
k	Conduction heat transfer coefficient (W/m^{2}k)
σ	Stefan-Boltzmann constant
Subscripts	
ap	Aperture
av	Average
cv	Convection
cd	Conduction
ra	Radiation
a	Ambient
g	Glass
fi	Inlet fluid
i	Inlet

REFERENCES

1. Gorjian, Sh., Nemat-Zadeh, B., Eltrop, R.R. Shamshiri, L. and Amanlou, Y., "Solar photovoltaic power generation in Iran: Development, policies, and barriers", ***Renewable and Sustainable Energy Reviews***, Vol. 106, (2019), 110-123. (https://doi.org/10.1016/j.rser.2019.02.025).
2. Gorjian, Sh. and Ghobadian, B., "Solar desalination: A sustainable solution to water crisis in Iran", ***Renewable and Sustainable Energy Reviews***, Vol. 48, (2015), 571-584. (https://doi.org/10.1016/j.rser.2015.04.009).
3. Gorjian, Sh., Ghobadian, B., Ebadi, H., Ketabchi, F. and Khanmohammadi, S., "Applications of solar PV systems in desalination technologies", Photovoltaic solar energy conversion, Elsevier, Iran, (2020), 237-274. (https://doi.org/10.1016/B978-0-12-819610-6.00008-9).
4. Sharon, H., Reddy, K.S. and Gorjian, Sh., "Parametric investigation and year round performance of a novel passive multi-chamber vertical solar diffusion still: Energy, exergy and enviro-economic aspects", ***Solar Energy***, Vol. 211, (2020), 831-846. (https://doi.org/10.1016/j.solener.2020.10.016).
5. Hosseini, A., Banakar, A. and Gorjian, Sh., "Development and performance evaluation of an active solar distillation system integrated with a vacuum-type heat exchanger", ***Desalination***, Vol. 435, (2017), 45-59. (https://doi.org/10.1016/j.desal.2017.12.031).
6. Gorjian, Sh., Ebadi, H., Calise, F., Shukla, A. and Ingrao, C., "A review on recent advancements in performance enhancement techniques for low-temperature solar collectors", ***Energy Conversion Management***, Vol. 222, (2020a), 113246. (https://doi.org/10.1016/j.enconman.2020.113246).
7. Gorjian, Sh., Ghobadian, B., Tavakkoli-Hashjin, T. and Banakar, A., "Experimental performance evaluation of a stand-alone point-focus parabolic solar still", ***Desalination***, Vol. 352, (2014), 1-17. (https://doi.org/10.1016/j.desal.2014.08.005).
8. Gorjian, Sh. and Ghobadian, B., "Solar thermal power plants: Progress and prospects in Iran", ***Energy Procedia***, Vol. 75, (2015), 533-539. (https://doi.org/10.1016/j.egypro.2015.07.447).
9. Madadi, V., Tavakoli, T. and Rahimi, A., "Estimation of heat loss from a cylindrical cavity receiver based on simultaneous energy and exergy analyses", ***Journal of Non-Equilibrium Thermodynamics***, Vol. 40, No. 1, (2015), 49-61. (https://doi.org/10.1515/jnet-2014-0029).
10. Gorjian, Sh., Tavakkoli-Hashjin, T., Ghobadian, B. and Banakar, A., "A thermal performance evaluation of a medium-temperature point-focus solar collector using local weather data and artificial neural networks", ***International Journal of Green Energy***, Vol. 12, No. 5, (2015), 493-505. (https://doi.org/10.1080/15435075.2013.848405).
11. Arkian, A.H., Najafi, G.H., Gorjian, Sh., Loni, R., Bellos, E. and Yusaf, T., "Performance assessment of a solar dryer system using small parabolic dish and alumina/oil nanofluid: Simulation and experimental study", ***Energies***, Vol. 12, No. 24, (2019), 4747. (https://doi.org/10.3390/en12244747).
12. Loni, R., Askari-Asli-Ardeh, E., Ghobadian, B., Kasaeian, A.B. and Gorjian, Sh., "Thermodynamic analysis of a solar dish receiver using different nanofluids", ***Energy***, Vol. 133, (2017), 749-760. (https://doi.org/10.1016/j.energy.2017.05.016).
13. Pavlovic, S., Daabo, A.M., Bellos, E., Stefanovic, V., Mahmoud, S. and Al-Dadah, R.K., "Experimental and numerical investigation on the optical and thermal performance of solar parabolic dish and corrugated spiral cavity receiver", ***Journal of Cleaner Production***, Vol. 150, (2017), 75-92. (https://doi.org/10.1016/j.jclepro.2017.02.201).
14. Li, X., Dai, Y.J. and Wang, R.Z., "Performance investigation on solar thermal conversion of a conical cavity receiver employing a beam-down solar tower concentrator", ***Solar Energy***, Vol. 114, (2015), 134-151. (https://doi.org/10.1016/j.solener.2015.01.033).
15. Abdulrazzaq Alhsani, Z.I. and Al-Dulaimi, R.K.M., "Experimental analysis of solar dish concentrators with cylindrical, oval, and conical cavity receivers", ***International Journal of Renewable Energy Research***, Vol. 10, (2020), 591-600.
16. Pavlovic, S., Loni, R., Bellos, E., Vasiljević, D., Najafi, G. and Kasaeian, A., "Comparative study of spiral and conical cavity receivers for a solar dish collector", ***Energy Conversion and Management***, Vol. 178, (2018), 111-122. (https://doi.org/10.1016/j.enconman.2018.10.030).
17. Daabo, A.M., Mahmoud, S. and Al-Dadah, R.K., "The optical efficiency of three different geometries of a small scale cavity receiver for concentrated solar applications", ***Applied Energy***, Vol. 179, (2016), 1081-1096. (https://doi.org/10.1016/j.apenergy.2016.07.064).
18. Daabo, A.M., Mahmoud, S., Al-Dadah, R.K. and Ahmad, A., "Numerical investigation of pitch value on thermal performance of solar receiver for solar powered Brayton cycle application", ***Energy***, Vol. 119, (2017), 523-539. (https://doi.org/10.1016/j.energy.2016.12.085).
19. Daabo, A.M., Ahmad, A., Mahmoud, S. and Al-Dadah, R.K., "Parametric analysis of small scale cavity receiver with optimum shape for solar powered closed Brayton cycle applications", ***Applied Thermal Engineering***, Vol. 122, (2017), 626-641. (https://doi.org/10.1016/j.applthermaleng.2017.03.093).
20. Azzouzi, D., Boumeddane, B. and Abene, A., "Experimental and analytical thermal analysis of cylindrical cavity receiver for solar dish", ***Renewable Energy***, Vol. 106, (2017), 111-121. (https://doi.org/10.1016/j.renene.2016.12.102).
21. Loni, R., Kasaeian, A.B., Askari-Asli-Ardeh, E., Ghobadian, B. and Gorjian, Sh., "Experimental and numerical study on dish concentrator with cubical and cylindrical cavity receivers using thermal oil", ***Energy***, Vol. 154, (2018), 168-181. (https://doi.org/10.1016/j.energy.2018.04.102).
22. Singh, A.K. and Natarajan, S.K., "Comparative study of modified conical cavity receiver with other receivers for solar paraboloidal dish collector system", ***Research Square***, (2021). (https://doi.org/10.21203/rs.3.rs-237950/v1).
23. Yuan, Y., Xiaojie, L., Ziming, C., Fuqiang, W., Yong, S. and Heping, T., "Experimental investigation of thermal performance enhancement of cavity receiver with bottom surface interior convex", ***Applied Thermal Engineering***, Vol. 168, (2020). (https://doi.org/10.1016/j.applthermaleng.2019.114847).
24. Bopche, S., Rana, K. and Kumar, V., "Performance improvement of a modified cavity receiver for parabolic dish concentrator at medium and

high heat concentration", ***Solar Energy***, Vol. 209, (2020), 57-78. (https://doi.org/10.1016/j.solener.2020.08.089).

25. Bellos, E., Bousi, E., Tzivanidis, C. and Pavlovic, S., "Optical and thermal analysis of different cavity receiver designs for solar dish concentrators", ***Energy Conversion and Management: X***, Vol. 2, (2019), 100013. (https://doi.org/10.1016/j.ecmx.2019.100013).
26. Soltani, S., Bonyadi, M. and Madadi-Avargani, V., "A novel optical-thermal modeling of a parabolic dish collector with a helically baffled cylindrical cavity receiver", ***Energy***, Vol. 168, (2019), 88-98. (https://doi.org/10.1016/j.energy.2018.11.097).
27. Thirunavukkarasu, V. and Cheralathan, M., "An experimental study on energy and exergy performance of a spiral tube receiver for solar parabolic dish concentrator", ***Energy***, Vol. 192, (2020), 116635. (https://doi.org/10.1016/j.energy.2019.116635).
28. Wang, H., Huang, J., Song, M. and Yan, J., "Effects of receiver parameters on the optical performance of a fixed-focus Fresnel lens solar concentrator/cavity receiver system in solar cooker", ***Applied Energy***, Vol. 237, (2019), 70-82. (https://doi.org/10.1016/j.apenergy.2018.12.092).
29. Al-Dulaimi, R.K.M., "Experimental investigation of the receiver of a solar thermal dish collector with a dual layer, staggered tube arrangement, and multiscale diameter", ***Energy Exploration and Exploitation***, Vol. 38, No. 4, (2020), 1212-1227. (https://doi.org/10.1177/0144598719900658).
30. Loni, R., Askari-Asli-Ardeh, E., Ghobadian, B., Kasaeian, A.B., Gorjian, Sh, Najafi, G. and Evangelos, B., "Research and review study of solar dish concentrators with different nanofluids and different shapes of cavity receiver: Experimental tests", ***Renewable Energy***, Vol. 145, (2020), 783-804. (https://doi.org/10.1016/j.renene.2019.06.056).
31. Gavagnin, G., Sánchez, D., Martínez, G.S., Rodríguez, J.M. and Muñoz, A., "Cost analysis of solar thermal power generators based on parabolic dish and micro gas turbine: Manufacturing, transportation and installation", ***Applied Energy***, Vol. 194, (2017), 108-122. (https://doi.org/10.1016/j.apenergy.2017.02.052).
32. Pathak, A., Deshpande, K., Kurhe, N., Baste, P. and Jadkar, S., "Comfort cooling application using fixed focus solar parabolic dish concentrator integrated with double effect vapor absorption Machine", ***International Research Journal of Engineering and Technology***, Vol. 5, No. 3, (2018), 1875-1880. (https://www.irjet.net/archives/V5/i3/IRJET-V5I3424.pdf).
33. Xie, W.T., Dai, Y.J. and Wang, R.Z., "Numerical and experimental analysis of a point focus solar collector using high concentration imaging PMMA Fresnel lens", ***Energy Conversion and Management***, Vol. 52, No. 6, (2011), 2417-2426. (https://doi.org/10.1016/j.enconman.2010.12.048).
34. Çengel, Y.A. and Ghajar, A.J., Heat and mass transfer: Fundamentals and applications, McGraw Hill, Turkey, (2007), 432-522. (https://www.mheducation.com).
35. ROCKWOOL stone wool insulation. (https://www.rockwool.com/group/).
36. Kirkup, L. and Frenkel, B., An introduction to unceratinty measurement using the GUM, Calculation of unceratinty, Cambridge University Press, Sydney, (2006), 97-125. (https://doi.org/10.1017/CBO9780511755538).
37. Yang S.M. and Tao, W.Q.B.Z., Heat transfer, Higher Education Press, (2000). (https://www.amazon.com/Transfer-third-Higher-Education-Chinese/dp/7040066939).
38. Jilte, R.D., Kedare, S.B. and Nayak, J.K., "Investigation on convective heat losses from solar cavities under wind conditions", ***Energy Procedia***, Vol. 57, (2014), 437-446. (https://doi.org/10.1016/j.egypro.2014.10.197).
39. Prakash, M., Kedare, S.B. and Nayak, J.K., "Investigations on heat losses from a solar cavity receiver", ***Solar Energy***, Vol. 83, No. 2, (2009), 150-170. (https://doi.org/10.1016/j.solener.2008.07.011).
40. Jilte, R.D., Kedare, S.B. and Nayak, J.K., "Natural convection and radiation heat loss from open cavities of different shapes and sizes used with dish concentrator", ***Mechanical Engineering Research***, Vol. 3, No. 1, (2013), 25-43. (https://doi.org/10.5539/mer.v3n1p25).
41. Mawire, A. and Taole, S.H., "Experimental energy and exergy performance of a solar receiver for a domestic parabolic dish concentrator for teaching purposes", ***Energy for Sustainable Development***, Vol. 19, (2014), 162-169. (https://doi.org/10.1016/j.esd.2014.01.004).